AJRCCM Articles in Press. Published on 18-May-2019 as 10.1164/rccm.201812-2322OC

Lung computational models and the role of the small airways in asthma

[1]Brody H. Foy[¥], [2]Marcia Soares[¥], [1,3]Rafel Bordas, [2]Matthew Richardson, [2]Alex Bell, [2]Amisha Singapuri, [2]Beverley Hargadon, [2]Christopher Brightling, [4]Kelly Burrowes, [1]David Kay, [5]John Owers-Bradley, [2]Salman Siddiqui

[¥]These authors contributed equally to the manuscript

Author Information

[1]Department of Computer Science, University of Oxford, Oxfordshire, United Kingdom.

[2]College of Life Sciences and NIHR Biomedical Research Centre: Respiratory Theme, University of Leicester, United Kingdom.

[3] Roxar Software Solutions, Oxford

[4]Department of Chemical and Materials Engineering, University of Auckland, Auckland, New Zealand.

[5]School of Physics and Astronomy, University of Nottingham, United Kingdom.

***Corresponding Author**

Professor Salman Siddiqui, NIHR Respiratory Biomedical Research Centre: Respiratory Theme and Department of Respiratory Sciences, University of Leicester. Glenfield Hospital, Leicester, LE3 9QP.

T: 0116 256 3841

E: ss338@le.ac.uk

FUNDING & ACKNOWLEDGEMENTS

Supported by grants from and National Institute for Health Research (NIHR) Leicester Biomedical Research Centre: Respiratory Theme (grant agreement no.RM65G0113), the East Midlands Comprehensive Clinical Research Network and EU FP7 AirPROM project (grant agreement no. 270194), unrestricted grant from the Chiesi Onulus Foundation (Validation of Particle in Exhaled Air (PEx) as a Novel Matrix for Non-Invasive Detection of Small Airways Disease in Asthma). BF is funded by the Rhodes Trust. The views expressed are those of the authors and not necessarily those of the NHS, the NIHR or the Department of Health. Some components of **Figure 1** were created (with permission) using stock photos from freepik.com

AUTHOR CONTRIBUTIONS

BF developed and implemented the computational modelling pipeline, analysed model outputs, co-wrote the manuscript and provided scientific critique of the data.

MS performed and analysed impulse oscillometry and clinical data in the clinical study population. Co-wrote the manuscript with BF and SS and provided a scientific critique of the data.

RB helped design and develop the computational modelling pipeline. Reviewed the manuscript and provided scientific critique of the data.

MR performed the pooled clinical trial statistical analyses.

AB constructed figure 1, reviewed the manuscript and provided a scientific critique of the data.

AJRCCM Articles in Press. Published on 18-May-2019 as 10.1164/rccm.201812-2322OC

AS and BH supported clinical patient recruitment in the observational cohorts and the trials.

CEB coordinated the AirPROM-FP7 consortium, was the chief investigator of the observational cohort and the clinical trials and reviewed the manuscript and provided a scientific critique of the data.

KB helped develop and implement the computational modelling pipeline, co-wrote the manuscript with SS and MS, and provided scientific critique of the data.

DK helped design and conceive of the overall study, supervised the development of the computational modelling pipeline, reviewed the manuscript and provided a scientific critique of the data.

SS conceived the study, helped secure funding for the study with CEB, supervised the development of the modelling (computational and statistical) and key modelling questions, co-wrote the manuscript and provided a scientific critique of the data

RUNNING HEAD

Computational models provide insight into asthma

SUBJECT CATEGORY

8.21 Modelling: Structure Function Relationships

ABSTRACT

RATIONALE: Asthma is characterised by disease within the small airways. Several studies have suggested that forced oscillation technique derived resistance at 5Hz minus 20Hz (R5-R20) is measure of small airways disease, however there has been limited validation of this measurement to date.

METHODS: Patient based complete conducting airway models were generated from CT scans to simulate the impact of different degrees of airway narrowing at different levels of the airway tree on forced oscillation R5-R20 (n=31). The computational models were coupled with regression models in an asthmatic cohort (n=177), to simulate the impact of small airway narrowing on asthma control and quality of life. The computational models were used to predict the impact on small airway narrowing of type-2 targeting biologics using pooled data from two similarly design randomised placebo control biologic trials (n=137).

RESULTS: Simulations demonstrated that narrowing of the small airways had a greater impact on R5-R20 than narrowing of the larger airways and was associated (above a threshold of approximately 40% narrowing) with marked deterioration in both asthma control and asthma quality of life, above the minimal clinical important difference. The observed treatment effect on R5-R20 in the pooled trials equated to a predicted small airway narrowing reversal of approximately 40%.

CONCLUSIONS: We have demonstrated using computational modelling that forced oscillation R5-R20 is a direct measure of anatomical narrowing in the small airways, that small airway narrowing has a marked impact on both asthma control and quality of life and may be modified

AJRCCM Articles in Press. Published on 18-May-2019 as 10.1164/rccm.201812-2322OC

by biologics.

WORD COUNT: 248

KEY WORDS: Asthma, Forced Oscillation Technique, Small Airways, Imaging, Computational Modelling, Integrative Modelling.

CLINICAL IMPLICATIONS

FOT measured low-high frequency resistive difference (R5-R20) was found to be a sensitive and clinically valuable marker of small airways disease.

CAPSULE SUMMARY

Coupling of computational airway models with statistical models has demonstrated that the forced oscillation measure R5-R20, is a sensitive to anatomical small airways disease and the models predict that narrowing of the small airways is associated with worsening asthma control and quality of life and may be modified by biologics.

ABBREVIATIONS

ACQ: Asthma control questionnaire

AQLQ: Asthma quality of life questionnaire

CT: Computed tomography

FOT: Forced oscillation technique

FRC: Functional residual capacity

GINA: Global initiative for asthma

IOS: Impulse Oscillometry

LLN: Lower limit of normal

MRI: Magnetic resonance imaging

PET: Positron emission tomography

R5: Resistance at 5 Hz

R20: Resistance at 20 Hz

R5-R20: Resistance at 5 Hz minus resistance at 20 Hz

SD: Standardised residual

SO: Strahler order

TLC: Total lung capacity

AJRCCM Articles in Press. Published on 18-May-2019 as 10.1164/rccm.201812-2322OC

INTRODUCTION

Asthma is a complex chronic inflammatory disease that involves both central and small airways [1-2]. Multiple lines of evidence suggest that within asthmatics, the small airways are dysfunctional [3], inflamed [4] and damaged [5]. Several *in vivo* imaging approaches have been utilised to study the small airways, including hyperpolarised gas, magnetic resonance imaging (MRI), and computed tomography (CT) imaging [6-7]. These studies have demonstrated that spatial disease in the small airways captured by both MRI and CT of the lungs may be adequately reflected in more simple measures of small airways disease using the forced oscillation technique (FOT).

FOT is a simple technique that perturbs the respiratory system during tidal breathing, by using a series of pressure oscillations, over a range of frequencies (typically 5-35Hz), applied at the mouth. Due to the lack of a required breathing manoeuvre, the FOT can be easily deployed across age groups, from young children, to the elderly. This suggests that it may be a suitable and clinically applicable tool for the measurement of small airways disease in adults and children with asthma [8]. The change in resistance from low to high frequency ranges (e.g. resistance at 5Hz minus 20Hz; R5-R20), is often suggested as a putative marker of small airways obstruction and has been shown to predict loss of asthma control in children [9]. This measure has also been shown to correlate with measures of small airway inflammation [10], exacerbations [11], and response to inhaled corticosteroids, including small particle formulations in adult asthma [12-14]. Recently, a multinational study of small airways dysfunction markers in adult asthma identified that IOS-measured R5-R20 was the most strongly correlated marker of small airways disease, of several small airway physiological markers. Furthermore 42% of the adult asthma population

demonstrated an abnormal R5-R20 measurement. These observations provide strong evidence that FOT derived R5-R20 is a useful clinical tool to identify small airways disease [15].

However, despite these observational studies the precise association between small airway anatomical narrowing and R5-R20 is poorly understood. Furthermore, the impact of small airway narrowing on asthma control, and quality of life has yet to be established.

Within this study, we hypothesised that: (i) anatomical disease within small airways (≤ 2mm in diameter) is a critical determinant of forced oscillation derived R5-R20 whilst accounting for relevant confounders and that R5-R20 and that (ii) anatomical narrowing of the small airways would be predicted to have a significant impact on both asthma control and quality of life.(iii) We also attempted to predict the impact of anti-inflammatory biologics targeting type 2 inflammation on small airway narrowing.

To investigate these hypotheses, we collected and analysed data from a variety of different sources. Our approach utilises patient-based computational modelling of the FOT [16]; and statistical regression models that link R5-R20 to asthma control and quality of life. Finally *post hoc* evaluation of existing placebo controlled clinical trial data was used to estimate the likely impact of anti-inflammatory biologics on small airway narrowing. The overarching concept of the study is outlined visually in **Figure 1**.

Some of the results of these studies have been previously reported in the form of an abstract[17].

AJRCCM Articles in Press. Published on 18-May-2019 as 10.1164/rccm.201812-2322OC

METHODS

Results within this study were created through combined analysis of three separate data sources: (i) a large asthmatic cohort, (ii) a smaller computational modelling cohort, and (ii) pooled clinical trial cohorts.

(i) Bio-statistical modelling cohort

An adult asthmatic cohort (n=177), was recruited from Glenfield Hospital, in Leicester, UK. Current smokers, and patients with a history of ≥ 10 pack years were excluded. Asthma was diagnosed by a physician, according to current British Thoracic Society guidelines [18], with severity defined according to the Global Initiative for Asthma (GINA) treatment intensity steps [19]. Details of the clinical study protocol are outlined in the **online supplement**, but in brief, participants attended for up to two visits, and underwent: Evaluation with asthma questionnaires for control and quality of life (ACQ-6 and AQLQ), and exacerbation frequency [20-21]; post bronchodilator impulse oscillometry (IOS), using a Jaeger MasterScreen [22]; and spirometry, according to European Respiratory Society (ERS) standards [23].

The study protocol for the recruitment and assessments in the two studies above was approved by the National Research Ethics Committee – East Midlands Leicester (approval number 08/H0406/189] and all subjects gave their written informed consent.

The data collected from this cohort was used to create a statistical regression linking R5-R20 to ACQ, and AQLQ. The linear regression was calculated using a stepwise algorithm, and incorporated GINA treatment intensity, age, sex, smoking exposure in pack years and spirometry measured forced-vital capacity (FVC) and forced expiratory volume/forced vital capacity ratio

(FEV_1/FVC) as potential confounding variables. Discriminatory variables were retained by the stepwise regression model and include as independent predictors as a means of adjustment.

(ii) Computational modelling cohort

A subset of 20 of the 177 asthmatic adults [(9 female, 11 male), who consented to participate in a CT imaging sub-study were selected at random from the cohort of 177 patients, and 11 healthy controls were recruited for imaging. Full details of the CT protocol are outlined in the original study [15]. All imaging was performed post-bronchodilator. Clinical characteristics of this cohort were well matched to the controls within the cohort and similar to patients with preserved spirometry in the overall cohort (Table 1 supplementary material) and well matched to the 11 control subjects. GINA treatment step 3[3: 4] and R5-R20 0.03[0.01:0.11] Kpa.s.L-1], age 59[47:65] years alongside 11 age matched healthy volunteers (6 female, 5 male), R5-R20 0.03 [0.02:0.06] Kpa.s.L-1) and age 59[43:66] years. Healthy subjects had no prior history of respiratory disease, normal spirometry and < 10 pack years smoking history.

- Creation of patient-based airway models

From each of the 31 inspiratory CT scans, a patient-based virtual airway structure was derived, by extracting centrelines of the central airways (to generation 6-10) and using a recursive algorithm [24] to grow the remainder of the conducting zone (to an average generation 16), within the identified lobar boundaries. The branch radii were scaled from total lung capacity (TLC)

AJRCCM Articles in Press. Published on 18-May-2019 as 10.1164/rccm.201812-2322OC

down to functional residual capacity (FRC) using Lambert's data [25]. Each patient-based virtual lung consisted of 30,000-100,000 branches, with the entire set being originally presented by Bordas *et al.*[16]. Within the original study, details of the structures were compared to histological data, with key features (radii, branch-lengths, etc.) lying within physiologically reasonable bounds[16].

- Computational model of the forced oscillation technique

The FOT was simulated using an electrical-circuit analogous model [26], with full details presented in the **online supplement**. In short, impedance of each airway branch was approximated using the wave-equation [27]. Total lung impedance was calculated by summing branch impedances in series and parallel, with each terminal bronchiole being subtended by a viscoelastic acinar model. This impedance was then added in series to contributions from the chest wall, trachea and glottis, and in parallel to contributions from cheek and upper airway shunting, all of which were parameterised using experimental data from the literature [28,29]. All simulations were performed in MATLAB.

Alongside simulating resistance in all patient-based structures, simulations were also performed in one of the structures derived from a healthy control, after application of artificial airway constrictions. Constrictions were applied by reducing branch radii in the structure by a fixed percentage (homogeneous) or drawing the reduction percentage from a normal distribution with a fixed mean (heterogeneous). Constrictions were either applied to all branches of a given Strahler order (marker of depth, 1 = terminal bronchiole, 12 = trachea), or to the small airways (orders 1-6) or large airways (7-10).

(iii) Clinical trial populations

To provide information on therapeutic intervention, we identified two similarly designed three-month duration anti-inflammatory randomised double-blind placebo-controlled phase II trials, in moderate-severe uncontrolled asthma. Both trials have been previously reported [30,31], and evaluated known targets relevant to asthma pathology in the small airways (IL-13 (n= 76) and the CRTH2 receptor DP2 (n=61)) with systemic therapies that would be expected to engage with their target in the small airways

Both trials used FOT-measured R5-R20 as an exploratory outcome, alongside ACQ, as an asthma control measure. Total cohort size (n=137) was chosen to provide 90% power for identification of a clinically meaningful change in R5-R20 of 0.03 $kPa.s.L^{-1}$ [12-14, 32-34], with details given in the online supplement.

Combined analysis procedure for model integration

The procedure for systematically and jointly analysing the various data sources is as follows. Resistance was simulated on each patient-based structure and compared against clinical measurements for validation. Then, model simulations were used to analyse the response of R5-R20 to small and large airway constrictions. These results were compared to clinical stratifications seen in the larger asthmatic cohort. A regression model, derived from the larger cohort, was used to link R5-R20 to ACQ and AQLQ, allowing for improved result interpretability. The combined model was then used to link biologic therapy results to changes in small airway narrowing and asthma control.

Statistical analysis

AJRCCM Articles in Press. Published on 18-May-2019 as 10.1164/rccm.201812-2322OC

Statistical analysis was performed using SAS 9.4, Prism 7, and MATLAB. A *p*-value of <0.05 was taken as the threshold for statistical significance. Comparisons across groups were performed using one-way ANOVA for parametric data or Kruskal–Wallis test for nonparametric data, and Fisher's exact test or the chi-squared test for proportions. Bonferroni/Dunn corrections for multiple comparisons were used as appropriate. Correlations between continuous variables were calculated using Pearson's correlation coefficient *(R*). We considered that FOT parameters were abnormally elevated when above 100% predicted of 95th percentile predicted value from the KORA cohort [35].

RESULTS

Identification of small airways within the patient-based lung structures

Airway depth within the patient-based lung structures was annotated using Strahler order (SO - the number of branches from a given location to the nearest terminal bronchiole), a standardized method for describing branching networks [16]. SO 1 refers to the terminal bronchioles, and on average, SO 12 to the trachea. Across the set of 31 structures the mean (std) airway diameter at SO 7 was 2.12mm (0.28 mm^2), and at SO 6 was 1.39mm (0.21mm^2), meaning orders 1-6 are treated as the small airways, and orders 7 and up as the large airways.

Correlation of simulated and clinical resistance measurements.

Within **Figure 2a-b**, we compare simulated (without artificial airway constriction) and clinically measured R5 and R20, across the 31 subjects who underwent CT imaging. As the figure shows, there is a moderate correlation [R^2 (R5 = 0.35, $p < 0.05$); R^2 (R20 = 0.27, $p < 0.05$)] between simulated and clinical data, with only one significant outlier. The correlation of simulated and clinically measured R5-R20 was modest, and individual R5 and R20 correlation errors were additive (data now shown).

Sensitivity of R5-R20 to small airways constriction

Within **Figure 2c-f,** we illustrate the simulated response of R5-R20 to various types of artificial airway constrictions applied to a structure based off a healthy control. Panels **2c-d** illustrate how R5-R20 responds to constriction, in both the presence and absence of heterogeneity (as defined in methods). In both cases R5-R20 responds sensitively to mild constriction, with the response being amplified as constriction increases. Significantly, a larger response is seen when constricting small airways (SO 1-6) than large airways. Additional simulations confirmed that 5Hz-20Hz was the

AJRCCM Articles in Press. Published on 18-May-2019 as 10.1164/rccm.201812-2322OC

optimal difference for detection of small airways disease, though 5Hz-25Hz was similarly effective **(Figure OS.3).**

The response to small airway constriction is also illustrated in panels **2e-f**. As shown, constriction of the small airways consistently produced larger responses than constriction of the large airways, regardless of whether constrictions were homogeneous or heterogeneous. Taking care to note the different axis scales used for R5 and R5-R20, the results clearly illustrate a larger relative increase in R5-R20 when comparing large and small airway constriction, than in R5. These conclusions were the same when using other types of constriction distributions **(online supplement)**.

To further illustrate this sensitivity, within **Figure 3** we show the relative contribution of the small airways, large airways, and cheek shunting, to R5 and R20, at baseline, and under mild (20%) and severe (50%) constriction, imposed uniformly on the small airways. In all three cases, R5 was dominated by small airway contributions more than R20. Furthermore, in the presence of severe airway constriction, the model derived R5-R20 (0.08 $kPa.s.L^{-1}$) was similar to the median reported R5-R20 for asthmatics in our cross-sectional cohort (0.09 $kPa.s.L^{-1}$, **table OS.1**), suggesting that the models are generating physiologically relevant values.

Large asthmatic cohort stratification based on R5-R20

Within **Figure 4,** we evaluate the prevalence of small airways dysfunction in the large asthmatic cohort, measured using R5-R20, and compared to spirometric values. The cohort was broken into three sub-groups, based upon (i) a low forced vital capacity < the lower limit f normal (LLN)[32], (ii) an abnormal FEV_1/FVC < LLN, and (ii) normal spirometry (both FEV1≥ LLN and FVC≥

LLN) outputs. (clinical interpretation and statistical summaries of the data underlying **Figure 4** are provided in the **online supplementary materials**).

Associating R5-R20 and small airway narrowing with patient outcomes

To allow for contextualization of R5-R20 in terms of reported patient outcomes, a linear regression model was built from the large asthmatic cohort data, to allow for prediction of asthma control (ACQ-6), and quality of life (AQLQ), based on patient R5-R20. This was done using a series of potential confounding independent variables (age, sex, GINA treatment intensity, FVC, FEV_1/FVC, and smoking exposure in pack-years). Details of the regression model are summarized in the **Table 1.**

Within **Figure 5,** we illustrate the potential value of the regression model, by transforming the R5-R20 values in **Figure 2e-f,** to ACQ and AQLQ values, using a 95% confidence interval on the regression coefficients for R5-R20. These results illustrate that deterioration in asthma control and quality of life occurs much more rapidly under constriction of the small airways than the large airways. Starting from a mild constricted state (20% constriction), small increases to constriction (moving from 20% to 40% constriction) would be expected to yield clinically relevant changes (> 0.5 units) in both ACQ and AQLQ.

Linking small airway changes to treatment outcomes

Having established that R5-R20 is sensitive to small airways disease, and contextualizing this in terms of patient related outcome measures, we seek to further evaluate these results in the context of clinical trial measured treatment outcomes. As shown in **Table 2**, the pooled treatment effect [95% CI] of two anti-inflammatory therapies [30-31] on R5-R20 was -0.038kPa.s.L^{-1} [-0.05:-0.03, $p < 0.0001$], comparative to placebo. Based on the results in **Figures 2-3**, we estimate that this

AJRCCM Articles in Press. Published on 18-May-2019 as 10.1164/rccm.201812-2322OC

treatment effect would be equivalent to a 35% [20-50%] reduction in small airway constriction, in the presence of moderate small airways dysfunction.

Within **Table 2,** we present the pooled estimate of treatment effect on ACQ (approximate only, as the two studies used different ACQ variants), as -0.19 (-0.26:-0.11, $p<0.0001$). We note that the predicted change in ACQ (from our model) based on the illustrated change in R5-R20 would be -0.08 (-0.03:-0.19), which is consistent with the actual change. This is particularly noteworthy given the regression model was derived from a cohort independent of the clinical trials.

DISCUSSION

Within this study, we have used a combination of computational modelling on patient-based lung structures to identify that low-high frequency resistive difference (R5-R20) is a clear marker of small airways anatomical constriction, and is strongly associated with patient outcome measures ACQ and AQLQ. Furthermore using our models, we have demonstrated that narrowing above a threshold of 40% in the small airways generates clinical important changes in asthma control and quality of life and that this effect is equivalent to the predicted narrowing reversal that would be expected with anti-inflammatory biologics based upon the observed treatment effects on R5-R20.

The validation of the computational lung impedance model, presented in **Figure 2a-b**, provides the largest (to our knowledge) patient-based validation of this model seen to date within the literature. The model that we have used has been used for large varieties of investigations within the literature [26,28,37,38]. Given this, this study helps provide validation to many prior results, built upon the theoretical foundations of the model.

Our results add further credence to the mounting evidence supporting R5-R20 as a robust small airways detection tool. The recent multinational ATLANTIS trial identified that R5-R20 was one of the key physiological determinants of small airways disease in asthma [15]. Furthermore, a recent study in COPD has linked anatomical narrowing of airways generations 7-9 measured with bronchoscopic optical coherence tomography with R5-R20 [39]. Taken together our observations provide further evidence supporting the validity of the claim that R5-R20 is a physiological marker of small airways disease.

The results within this manuscript used 5Hz and 20Hz as the low and high frequency points for calculating resistive difference. This choice was made primarily due to the prevalence of R5-R20

AJRCCM Articles in Press. Published on 18-May-2019 as 10.1164/rccm.201812-2322OC

within the literature, comparative to other index choices. However, for completeness, within the **online supplement** we also present a brief analysis of a variety of choices of low and high points within the frequency range 5-35Hz. Through this analysis it is shown that R5-R20 is significantly more sensitive to small airways constriction than most other frequency choices.

The results in **Figures 2-3** clearly illustrate the value of low-high frequency resistive difference as a marker of small airways dysfunction. This conclusion is furthered by the results in **Figure 4**, which suggest that R5-R20 may stratify small airways disease, even in the presence of normal spirometric values. This compares well to other results in the literature [3,15,40] which have suggested the value of R5-R20 as a predictor of small airways dysfunction.

The analysis in **Figures 2-4** becomes more meaningful when interpreted in context of the underlying statistical relationship between R5-R20, ACQ, and AQLQ, as in **Figure 5**. This figure illustrates that small airways constriction leads to significantly larger reductions in asthma control and quality of life, than large airway constrictions, suggesting that a major determinant of asthma control and quality of life may be disease within the small airways in keeping with the results of the multinational ATLANTIS study [15]. The results in **Figure 5** suggest that the initial effect of small airway constriction on ACQ and AQLQ is quite minimal, with an approximate 40% reduction in small airway radii needed to create the minimal clinically important change (0.5 units). However, once disease is already present, smaller increases in disease severity appear to lead to much larger degradations in patient quality of life (e.g. moving from 50% to 60% constriction decreases AQLQ from approximately 5 to 3.5).

The ability to more precisely connect morphological changes in lung structure with clinical pulmonary measurements, and patient quality of life assessments is a truly valuable and novel contribution. This is further illustrated by connecting these results to the clinical trial results in

Table 2. The pooled estimate effect on R5-R20 had a 95% confidence interval of -0.05:-0.03 $kPa.s.L^{-1}$. Interpreting this in terms of **Figure 2e-f**, allows for an approximate interpretation of this change in context of the underlying small airway morphology. Reductions in R5-R20 of this magnitude could be interpreted as being driven by a 35% [20:50%] reduction in mean constriction severity of the small airways (a transition from mild/severe constriction towards a healthy state). Importantly, the statistical regression relationship was also able to accurately predict the observed treatment effect on ACQ, from the observed effect on R5-R20, giving further confidence to the results.

Study limitations

The concordance between simulated and clinically measured R5-R20 in our study was modest but illustrates the ability of the model to distinguish between high and low responses. Part of the error between simulated and clinical values may be due to the use of mean population data for the shunting and tracheal impedances, and the use of a simple constant-phase model [(26)], for respiratory zone contributions.

Within recent work by this group [(17)], CT voxel deformation data was used to improve structural accuracy of the virtual lungs. For a subset of the virtual lungs in this study, this process improved the R^2 between simulated and clinical R5 from 0.61 to 0.78. This suggests that a significant degree of noise in the model, may simply be due to limitations in imaging accuracy.

It should be noted that the computationalmodelling cohort was comprised of a randomly selected subset of the larger clinical cohort. This subset had R5-R20 values that spanned the range of the

AJRCCM Articles in Press. Published on 18-May-2019 as 10.1164/rccm.201812-2322OC

larger cohort, and due to the randomized selection process, we do not believe that this subset biases the results.

Finally, the simulated results in this manuscript relied on enforcing constricting patterns either homogeneously or through a normal distribution. For completeness, within the **online supplement**, we investigate the effect of skew-normally distributed airway constrictions on R5-R20, showing qualitatively similar results to those contained within the main manuscript.

SUMMARY

These findings illustrate a clear and consistent relationship between anatomical small airways disease, and lung impedance measurement R5-R20. Using a combination of patient-based computational modelling, large scale clinical assessment, and clinical trial data, this relationship can be linked to patient outcome measures, and be used to predict therapeutic intervention responses. Furthermore, this study stands as a prototype for the value of integrated computational-clinical approaches to understand the role of small airways disease in respiratory medicine.

WORD COUNT: 3500

REFERENCES

(1) Contoli M, *et al*. Do small airway abnormalities characterize asthma phenotypes? In search of proof. *Clin Exp Allergy.* **42**(8), 1150-60 (2012).

(2) Lipworth B, Manoharan A, Anderson W. Unlocking the quiet zone: the small airway asthma phenotype. *Lancet Respir Med*. **2**(6), 497-506 (2014).

(3) Usmani OS, Singh D, Spinola M, Bizzi A, Barnes PJ. The prevalence of small airways disease in adult asthma: A systematic literature review. *Respir Med*. **116**, 19-27 (2016).

(4) Hamid Q, Song Y, Kotsimbos TC, Minshall E, Bai TR, Hegele RG, Hogg JC. Inflammation of small airways in asthma. *J Allergy Clin Immunol*.**100**(1), 44-51 (1997).

(5) Hyde DM, Hamid Q, Irvin CG. Anatomy, pathology, and physiology of the tracheobronchial tree: emphasis on the distal airways. *J Allergy Clinical Immunol*. **124**(6):S72-7 (2009).

(6) Eddy RL, Westcott A, Maksym GN, Parraga G, Dandurand RJ. Oscillometry and pulmonary magnetic resonance imaging in asthma and COPD. Physiol Rep. 2019 Jan;7(1):e13955.

(7) Bell AJ, Foy BH, Richardson M, Singapuri A, Mirkes E, van den Berge M, Kay D, Brightling C, Gorban AN, Galbán CJ, Siddiqui S. Functional CT imaging for identification of the spatial determinants of small-airways disease in adults with asthma. J Allergy Clin Immunol. 2019 Jan 22. pii: S0091-6749(19)30087-9

AJRCCM Articles in Press. Published on 18-May-2019 as 10.1164/rccm.201812-2322OC

(8) Galant, SP, Komarow, HD, Shin HW, Siddiqui, S, & Lipworth B. The case for impulse oscillometry in the management of asthma in children and adults. *Annals of Allergy, Asthma & Immunology*. **118**(6), 664-671. (2017).

(9) Shi Y, Aledia AS, Galant SP, George SC. Peripheral airway impairment measured by oscillometry predicts loss of asthma control in children. *J Allergy Clin Immuno*, **131**(3):718-23 (2013).

(10) Williamson PA, Clearie K, Menzies D, Vaidyanathan S, Lipworth BJ. Assessment of small-airways disease using alveolar nitric oxide and impulse oscillometry in asthma and COPD. *Lung*, **189**(2):121-9 (2011).

(11) Gonem S, *et al*. Airway impedance entropy and exacerbations in severe asthma. *Eur Respir J*, **40**(5):1156-63 (2012).

(12) Hozawa S, Terada M, Hozawa M. Comparison of budesonide/formoterol Turbuhaler with fluticasone/salmeterol Diskus for treatment effects on small airway impairment and airway inflammation in patients with asthma. *Pulm pharmacol Ther*., **24**(5):571-6 (2011).

(13) Hozawa S, Terada M, Hozawa M. Comparison of the effects of budesonide/formoterol maintenance and reliever therapy with fluticasone/salmeterol fixed-dose treatment on airway inflammation and small airway impairment in patients who need to step-up from inhaled corticosteroid monotherapy. *Pulm Pharmacol Ther*, **27**(2):190-6 (2014).

(14) Hozawa S, Terada M, Haruta Y, Hozawa M. Comparison of early effects of budesonide/formoterol maintenance and reliever therapy with fluticasone furoate/vilanterol for

asthma patients requiring step-up from inhaled corticosteroid monotherapy. *Pulm Pharmacol Ther*, **37**:15-23 (2016).

(15) Postma DS, Brightling C, Baldi S, Van den Berge M, Fabbri LM, Gagnatelli A, Papi A, Van der Molen T, Rabe KF, Siddiqui S, Singh D, Nicolini G, Kraft M; ATLANTIS study group. Exploring the relevance and extent of small airways dysfunction in asthma (ATLANTIS): baseline data from a prospective cohort study. Lancet Respir Med. 2019 Mar 12. pii: S2213-2600(19)30049-9. doi: 10.1016/S2213-2600(19)30049-9.

(16) Bordas R, *et al*. Development and analysis of patient-based complete conducting airways models. PloS one, **10**(12):e0144105 (2015).

(17) Foy, B, Bell, A, Siddiqui, SH, Kay, D. Low frequency lung resistance is a global bronchoconstriction detection measure but is still sensitive to small airways disease. Poster presented at: American Thoracic Society Meeting; 2018 May 22-25; San Diego

(18) BTS/SIGN British Guideline on the Management of Asthma. British Thoracic Society/Scottish Intercollegiate Guidelines Network (2016). Available from: https://www.brit-thoracic.org.uk/standards-of-care/guidelines/btssign-british-guideline-on-the-management-of-asthma/. Accessed 1st July 2018.

(19) Global Initiative for Asthma (GINA). The global strategy for asthma management and prevention, 2017. Available from http://www.ginasthma.org. Accessed 1st July 2018.

(20) Juniper EF, Svensson K, Mörk AC, Ståhl E. Measurement properties and interpretation of three shortened versions of the asthma control questionnaire. *Respir Med*, **99**(5): 553-8 (2005).

AJRCCM Articles in Press. Published on 18-May-2019 as 10.1164/rccm.201812-2322OC

(21) Juniper EF, *et al*. Validation of a standardized version of the Asthma Quality of Life Questionnaire. *Chest,* **115**(5): 1265-1270 (1999).

(22) Oostveen E, *et al*. The forced oscillation technique in clinical practice: methodology, recommendations and future developments. *Eur Respir J*, **22**(6):1026-41 (2003).

(23) Miller MR, et al. Standardisation of spirometry. *Eur Respir J*, **26**(2):319-38 (2005).

(24) Tawhai, MH, *et al*. CT-based geometry analysis and finite element models of the human and ovine bronchial tree. *J Appl Physiol*, **97**(6), 2310-2321 (2004).

(25) Lambert RK, Wilson TA, Hyatt RE, Rodarte JR. A computational model for expiratory flow. *J Appl Physiol*, ***52***(1), 44-56 (1982).

(26) Lutchen KR., Gillis H. Relationship between heterogeneous changes in airway morphometry and lung resistance and elastance. *J Appl Physiol,* **83**(4), 1192-1201 (1997).

(27) Benade AH. On the propagation of sound waves in a cylindrical conduit. *J Acoust Soc Am*, **44**(2), 616-623 (1968).

(28) Bhatawadekar, SA, Leary D, Maksym GN. Modelling resistance and reactance with heterogeneous airway narrowing in mild to severe asthma. *Can J Physiol Pharmacol*, **93**(3), 207-214 (2015).

(29) Cauberghs M., Van de Woestijne, K. P. Mechanical properties of the upper airway. *J Appl Physiol*, **55**(2), 335-342 (1883).

(30) Gonem S, *et al*. Fevipiprant, a prostaglandin D2 receptor 2 antagonist, in patients with persistent eosinophilic asthma: a single-centre, randomised, double-blind, parallel-group, placebo-controlled trial. *Lancet Respir Med*, **4**(9):699-707 (2016).

(31) Russell R.J, *et al*. Effect of tralokinumab, an interleukin-13 neutralising monoclonal antibody, on eosinophilic airway inflammation in uncontrolled moderate-to-severe asthma (MESOS): a multicentre, double-blind, randomised, placebo-controlled phase 2 trial. *Lancet Respir Med* (2018). doi: 10.1016/S2213-2600(18)30201-7. [Epub ahead of print].

(32) Hoshino, M. Comparison of effectiveness in ciclesonide and fluticasone propionate on small airway function in mild asthma. *Allerg Int*, ***59***(1): 59-66 (2010).

(33) Yamaguchi, M, Niimi, A, Ueda, T, Takemura, M, Matsuoka, H, Jinnai, M, Otsuka, K, Oguma, T, Takeda, T, Ito, I, & Matsumoto H. Effect of inhaled corticosteroids on small airways in asthma: investigation using impulse oscillometry. *Pulm Pharm & Therap.* **22(4)**, 326-332.

(34) Gonem S, *et al*. Clinical significance of small airway obstruction markers in patients with asthma. *Clin Exp Allergy*, **44**(4):499-507 (2014)

(35) Schulz H, *et al*. Reference values of impulse oscillometric lung function indices in adults of advanced age. PloS one, **8**(5):e63366 (2013).

(36) Sorkness RL, *et al*. Lung function in adults with stable but severe asthma: air trapping and incomplete reversal of obstruction with bronchodilation. *J Appl Physiol*, **104**(2):394-403 (2008).

(37) Foy, BH, & Kay, D. A computational comparison of the multiple-breath washout and forced oscillation technique as markers of bronchoconstriction. *Resp Phys & NeuroBio,* **240**, 61-69. (2017)

AJRCCM Articles in Press. Published on 18-May-2019 as 10.1164/rccm.201812-2322OC

(38) Kaczka, DW, Ingenito, EP, Suki, B, & Lutchen, KR. Partitioning airway and lung tissue resistances in humans: effects of bronchoconstriction. *J Appl Physiol*, **82**(5), 1531-1541 (1997).

(39) Su, ZQ *et al*. Significances of spirometry and impulse oscillometry for detecting small airway disorders assessed with endobronchial optical coherence tomography in COPD. *Int J Chron Obstruct Pulmon Dis,***13**: 3031 (2018).

(40) van der Wiel, E, ten Hacken, NH, Postma, DS, & van den Berge, M. Small-airways dysfunction with respiratory symptoms and clinical features of asthma: a systematic review. *J Allerg Clin Immun*. **131.3**, 646-657. (2013).

COMPETING INTERESTS

BF, MS, RB, MR, AB, AS, BH, DK and JOB have no competing conflict of interests to declare. CEB has received funding as grants and or consultancy paid to his Institution from AZ, MedImmune, GSK, Novartis, Pfizer, Chiesi, Merck, Sanofi, Regeneron, 4DPharma, Glenmark, Gilead, PreP, Mologic, Gossamer, 3M, Roche, Genentech and BI.CEB is a member of the ERS, ATS and BTS severe asthma guidelines and a Director of the ERS Research Collaborations. SS has received funding as grants and or consultancy paid to his Institution from AZ, GSK, Novartis, Chiesi, Owlstone Medical, NAPP, Mundipharma and Boehringer Ingelheim. SS is a member of the ERS.

FIGURE LEGENDS

Figure 1: Diagram of the integrated modelling approach.

Legend to figure 1: The diagram shows many of the different clinical, statistical, and computational components that are used together in this integrated study. This includes the patient subset that underwent CT scans, leading to the creation of patient-based lung structures, and personalised FOT modelling; as well as the larger asthmatic cohort used to create regressive links between FOT outcomes, and more standardised asthmatic assessments. This integrative approach leads to a deeper understanding of the links between underlying physiology and patient outcomes.

Figure 2: Analysis of the response of simulated R5-R20 to airways constriction.

Legend to figure 2: The ability of the model to simulate healthy (black circles) and asthmatic (red squares) patient values is first shown, with R^2 values for (A) R5: 0.35, and (B) R20: 0.27, and strong statistical significance ($p < 0.05$) in both cases. In panels (C) and (D), the response of R5-R20 to homogeneous and heterogeneous constrictions at different depths (denoted by Strahler order) is given. In both cases, R5-R20 is seen to peak when constricting smaller airways (orders 1-6), and then decrease under upper airway constriction. The response of R5-R20 to small airways constriction is further illustrated by comparing homogeneous (E) and heterogeneous (F) constriction of all small airways (orders 1-6) and central airways (orders 7-12). A consistently stronger response is seen from the small airways. In panels (E) and (F) R5 (right axis) and R5-R20 (left axis) are both given, with R5 showing a larger response, but a smaller distinction (particularly comparative to baseline values) between small and central airway constriction.

AJRCCM Articles in Press. Published on 18-May-2019 as 10.1164/rccm.201812-2322OC

Figure 3: Relative contributions of small airways, central airways and upper airway/cheek shunting to R5 and R20.

Legend to figure 3: The simulated relative contributions are shown for a healthy subject, under mild constriction (20%), and severe constriction (50%) of all small airways, alongside the resistance and reactance curves from 2-35Hz. In all 3 cases, small airways contribute more significantly to R5 than R20, with the magnitude of this effect increasing with disease severity. This suggests that R5-R20 responds most strongly to small airways constriction.

Figure 4: Stratification of the clinical study population according to FVC Z score and FEV_1/FVC LLN.

Legend to figure 4: Stratification according to spirometry culminated in three different groups: gas trapping, Asthma/COPD overlap, early small airway disease. Pie charts show the percentage of patients in each group with R5-R20> 100% predicted, utilizing the 95th percentile KORA cohort quantile-quantile regression equations (Pie charts: white part corresponds to R5-R20>100% predicted and white part corresponds to R5-R20≤ 100% predicted). Further clinical details for each group can be found in the online supplement, Table OS.1.

Figure 5: Simulated response of ACQ and AQLQ to airways constriction.

Legend to Figure 5: The translation of the response of R5-R20 to small and central airways constriction, into ACQ and AQLQ, using regressive models from **Table 1**. Results were calculated using the mean regression parameter value for R5-R20 (black line), as well as the 95% confidence interval (coloured bands). For both ACQ and AQLQ, a much more severe response is seen under small airways constriction than central airways constriction, even after accounting for the uncertainty of the regression.

TABLES

Table 1: Regression models for ACQ and AQLQ.

AQLQ Model					
Effect	**Estimate**	**Standard Error**	**P-value**	**95% CI Lower Bound**	**95% CI Upper Bound**
Intercept	5.832	0.445	< 0.001	4.953	6.712
R5-R20 ($kPa.s.L^{-1}$)	-3.292	0.967	0.001	-5.202	-1.383
GINA (1-5)	-0.258	0.069	< 0.001	-0.394	-0.122
FVC (L)	0.199	0.090	0.028	0.021	0.377
ACQ-6 Model					
Effect	**Estimate**	**Standard Error**	**P-value**	**95% CI Lower Bound**	**95% CI Upper Bound**
Intercept	1.911	0.715	0.008	0.499	3.322
R5-R20 ($kPa.s.L^{-1}$)	2.195	0.787	0.006	0.640	3.749
GINA (1-5)	0.314	0.058	<0.001	0.199	0.429
Age (yrs)	-0.016	0.005	0.003	-0.027	-0.006
Pack-years (yrs)	0.018	0.008	0.033	0.001	0.034
Sex (Male)	0.378	0.145	0.01	0.091	0.665
FEV1/FVC	-0.016	0.007	0.026	-0.030	-0.002

Legend: Results of stepwise (forward selection) linear regression models. Dependent variables are AQLQ and ACQ. For AQLQ independent variables are R5-R20, GINA treatment step, and forced vital capacity (FVC). For ACQ model independent variables are R5-R20, GINA treatment step, age, pack-years (PYRS), sex, and FEV1/FVC.

AJRCCM Articles in Press. Published on 18-May-2019 as 10.1164/rccm.201812-2322OC

Table 2: Pooled clinical trial data using R5-R20, and ACQ as markers.

	Change from baseline to week 12		Treatment effect
	Tralokinumab (n = 36)	Placebo (n = 40)	
Change in ACQ-6	-0.96(0.14)¥	-0.87(0.14)¥	-0.08(0.20)§ p=0.67
Change in R5-R20 ($kPa.s.L^{-1}$)	-0.04 (0.02)¥	-0.01 (0.01)¥	-0.03 (0.02)§ p = 0.19
	Fevipiprant (n = 29)	Placebo (n = 32)	
Change in ACQ-7	-0.18(0.92)¥	0.14(0.96)¥	-0.32(0.24)§ p=0.19
Change in R5-R20 ($kPa.s.L^{-1}$)	-0.03 (0.11)¥	0.02 (0.11)¥	-0.05 (0.03)§ p = 0.11
	Pooled		
Pooled estimate change in ACQ	-0.612(0.62)¥	-0.42(0.64)¥	-0.19(0.21)§ p<0.0001 95% CI: -0.26 to -0.11
Pooled estimate change in R5-R20 ($kPa.s.L^{-1}$)	-0.034 (0.07)¥	0.002 (0.07)¥	-0.038 (0.024)§ p <0.0001 95% CI: -0.05 to -0.03

Legend for Table 1: ¥=mean (standard deviation), §=difference in means (standard error). Change and treatment effect on R5-R20 (Resistance at 5 HZ minus resistance at 20 Hz), and asthma control questionnaire (ACQ) of two three-month duration, anti-inflammatory, randomised double blind placebo controlled phase 2 trials in moderate-severe uncontrolled asthma, for both intervention and placebo (20-21). Pooled estimated treatment effect [95% CI] of the two anti-inflammatory therapies is shown. Note that for ACQ, the two treatments used different validated variants of the questionnaire (ACQ6, and ACQ7). Given this, the pooled estimate treatment effect for ACQ is intended as approximate only.

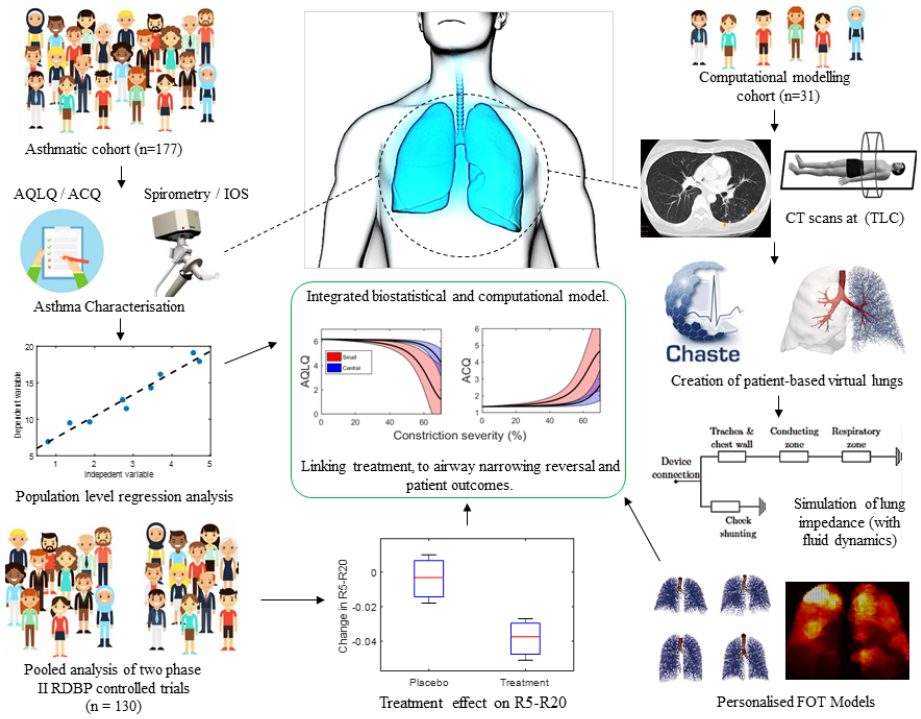

Figure 1: Diagram of the integrated modelling approach.
The diagram shows many of the different clinical, statistical, and computational components that are used together in this integrated study. This includes the patient subset that underwent CT scans, leading to the creation of patient-based lung structures, and personalised FOT modelling; as well as the larger asthmatic cohort used to create regressive links between FOT outcomes, and more standardised asthmatic assessments. This integrative approach leads to a deeper understanding of the links between underlying physiology and patient outcomes.

254x190mm (96 x 96 DPI)

AJRCCM Articles in Press. Published on 18-May-2019 as 10.1164/rccm.201812-2322OC

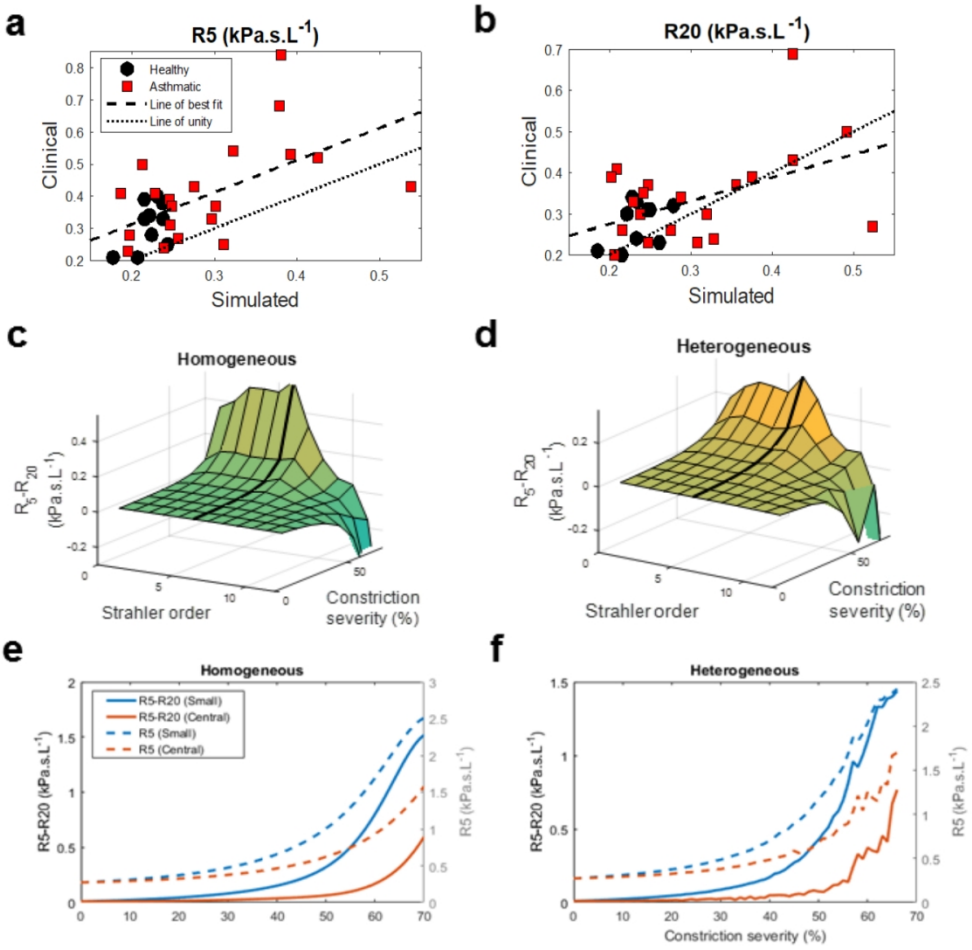

Figure 2: Analysis of the response of simulated R5-R20 to airways constriction.
The ability of the model to simulate healthy (black circles) and asthmatic (red squares) patient values is first shown, with R2 values for (A) R5: 0.35, and (B) R20: 0.27, and strong statistical significance ($p < 0.05$) in both cases. In panels (C) and (D), the response of R5-R20 to homogeneous and heterogeneous constrictions at different depths (denoted by Strahler order) is given. In both cases, R5-R20 is seen to peak when constricting smaller airways (orders 1-6), and then decrease under upper airway constriction. The response of R5-R20 to small airways constriction is further illustrated by comparing homogeneous (E) and heterogeneous (F) constriction of all small airways (orders 1-6) and central airways (orders 7-12). A consistently stronger response is seen from the small airways. In panels (E) and (F) R5 (right axis) and R5-R20 (left axis) are both given, with R5 showing a larger response, but a smaller distinction (particularly comparative to baseline values) between small and central airway constriction.

363x354mm (96 x 96 DPI)

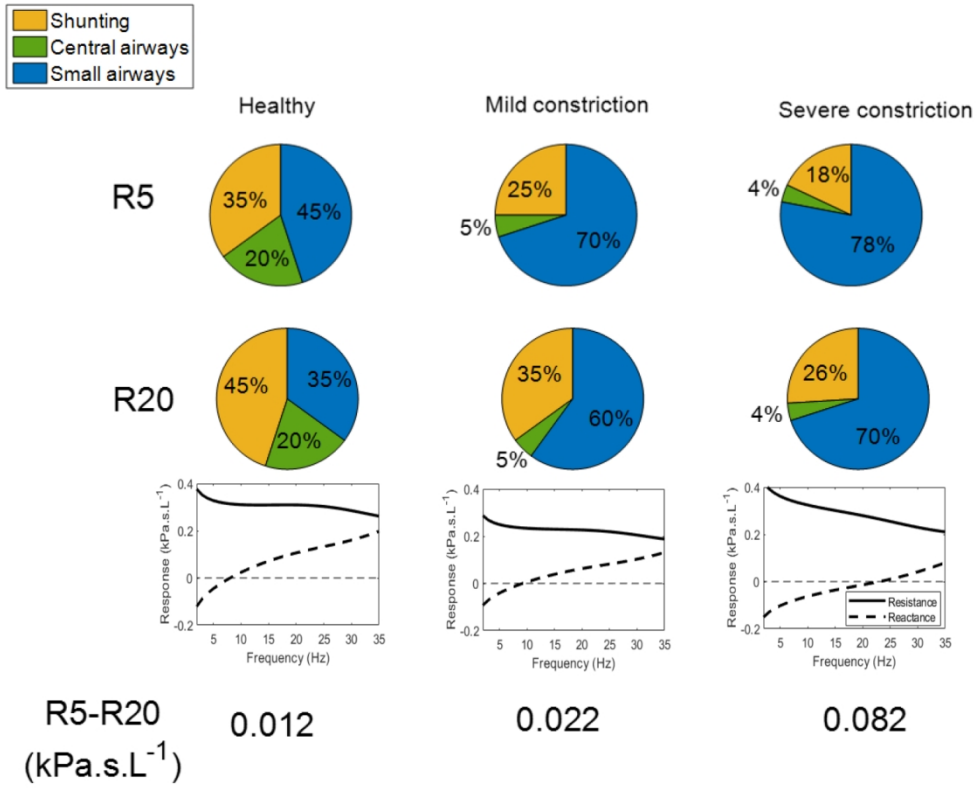

Figure 3: Relative contributions of small airways, central airways and upper airway/cheek shunting to R5 and R20.
The simulated relative contributions are shown for a healthy subject, under mild constriction (20%), and severe constriction (50%) of all small airways, alongside the resistance and reactance curves from 2-35Hz. In all 3 cases, small airways contribute more significantly to R5 than R20, with the magnitude of this effect increasing with disease severity. This suggests that R5-R20 responds most strongly to small airways constriction.

438x357mm (96 x 96 DPI)

AJRCCM Articles in Press. Published on 18-May-2019 as 10.1164/rccm.201812-2322OC

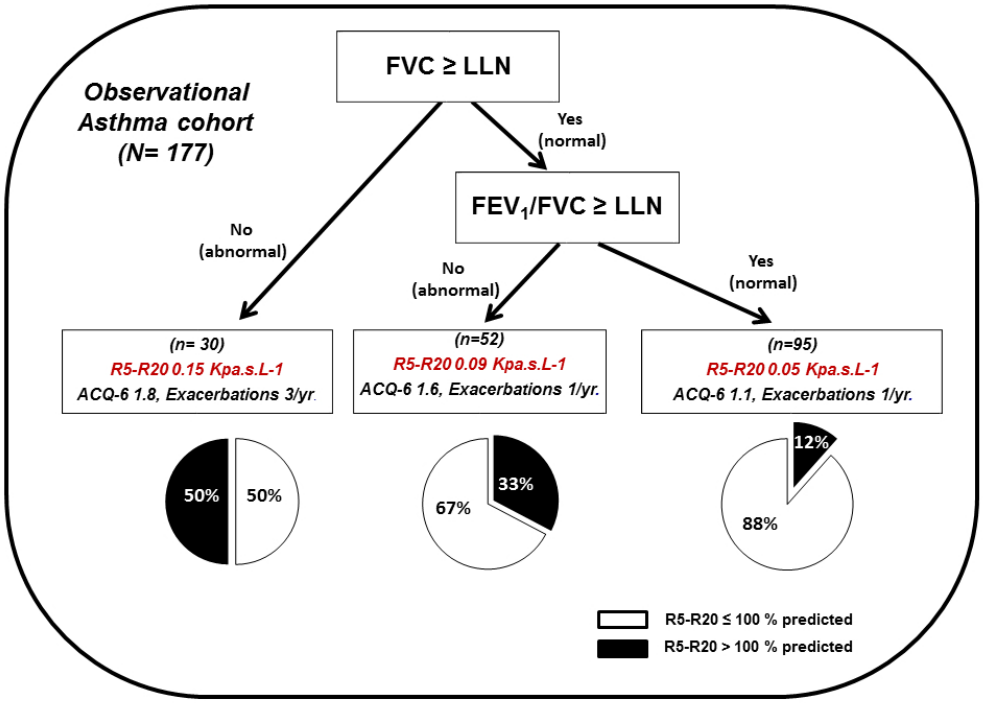

Figure 4: Stratification of the clinical study population according to FVC Z score and FEV1/FVC LLN. Stratification according to spirometry culminated in three different groups: gas trapping, Asthma/COPD overlap, early small airway disease. Pie charts show the percentage of patients in each group with R5-R20> 100% predicted, utilizing the 95th percentile KORA cohort quantile-quantile regression equations (Pie charts: white part corresponds to R5-R20>100% predicted and white part corresponds to R5-R20≤ 100% predicted). Further clinical details for each group can be found in the online supplement, Table OS.1.

202x152mm (120 x 120 DPI)

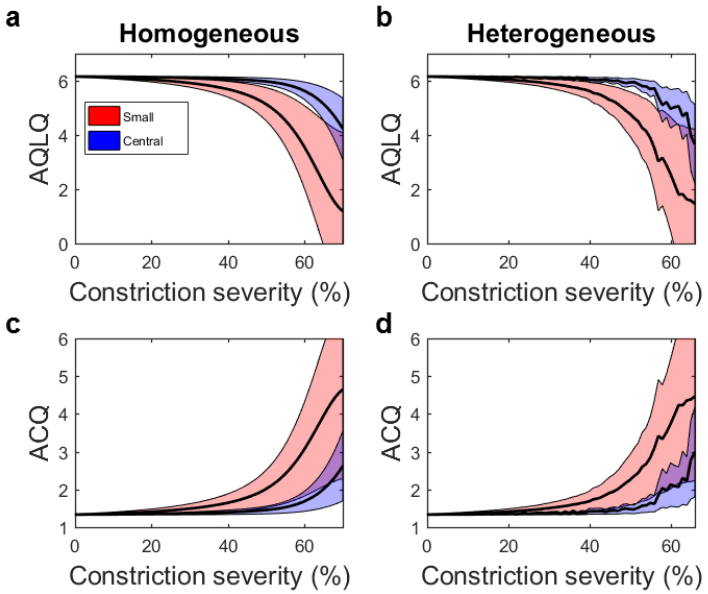

Figure 5: Simulated response of ACQ and AQLQ to airways constriction.
The translation of the response of R5-R20 to small and central airways constriction, into ACQ and AQLQ, using regressive models from Table 1. Results were calculated using the mean regression parameter value for R5-R20 (black line), as well as the 95% confidence interval (coloured bands). For both ACQ and AQLQ, a much more severe response is seen under small airways constriction than central airways constriction, even after accounting for the uncertainty of the regression.

254x190mm (96 x 96 DPI)

AJRCCM Articles in Press. Published on 18-May-2019 as 10.1164/rccm.201812-2322OC

ONLINE SUPPLEMENT: Lung computational models and the role of the small airways in asthma

Supplement 1: Clinical study protocol

Within the main study, data analysis was performed on clinical measurements taken from an asthmatic cohort. For brevity, details of the clinical data collection were omitted in the manuscript, these details are presented here.

A group of 177 asthmatic adults were recruited from Glenfield hospital, Leicester, UK. Current smokers, and patients with a history of $\geq$ 10 pack years were excluded. All participants attended for up to two visits (within a week), not less than six weeks following an asthma exacerbation. Physiological tests and CT [at both total lung capacity (TLC) and functional residual capacity (FRC)] were performed 15 minutes after administration of the short-acting bronchodilator via Volumatic: 400μg.

In addition to the collection of demographic and clinical details, six-point Juniper Asthma Control Questionnaire (ACQ-6) and standardised Asthma Quality of Life Questionnaire AQLQ [AQLQ(S)] [1-2] were completed. IOS was performed using a Jaeger MasterScreen (Viasys Healthcare GmbH, Hoechberg, Germany) [3] and spirometry, according to ATS/ERS standards [4].

IOS values are known to be associated with height, sex and age. Despite the lack of well-established reference values for IOS parameters from a large and mixed adult population, efforts have been taken place to address this need [5]. We utilised normative values appropriately adjusted for age, sex and height for IOS that have been developed in a large healthy Caucasian never smoking population of a similar median age to the asthma population in this study [6]. We

considered that impulse oscillometry parameters were abnormally elevated when above 100% predicted of 95th percentile predicted value from the KORA cohort.

For the therapeutic intervention cohorts, both studies used FOT-measured R5-R20 as an exploratory outcome, alongside ACQ as a measure of asthma control. We pooled the results of the trials as we estimated based upon previous anti-inflammatory inhaled steroid studies in asthma that to detect a 0.03 Kpa.s.L^{-1} change in R5-R20 [7-11], with a SD of 0.05 Kpa.s.L^{-1}[12], we would require and n =58 patients per group (116 patients in total) to have a 90% power and an α: 0.05.

Supplement 2. Outline of the computational lung impedance model

Within the study, we presented the results of simulations of lung impedance on a set of 1D structural representations of the lungs. For brevity full details of the model were omitted from the main manuscript, and are instead presented here.

All of the virtual, patient-based conducting zone lung structures (created through CT segmentation, and algorithmic generation[13-15]), are 1D in nature. To simulate lung impedance on these 1D structures, we use an electrical circuit analogous model, which is widely used within the literature[16-17]. This model assumes that each branch independently contributes to impedance, with total lung impedance being the additive result of series and parallel contributions from all branches in the network.

To approximate the impedance Z_j of a branch j, in response to a pressure pulse of frequency f, we use the model proposed by Benade[18] and Thurston[19]:

AJRCCM Articles in Press. Published on 18-May-2019 as 10.1164/rccm.201812-2322OC

$$Z_j = \left(i\frac{\omega\rho l_j}{\pi r_j^2}\right)\left(1-\frac{2\quad J_1(r_v\sqrt{-i})}{r_v\sqrt{-i}J_0(r_v\sqrt{-i})}\right)^{-1}, \qquad r_v = \left(\frac{\omega\rho}{\mu}\right)^{1/2} r_j$$

where ρ is the air density, μ is the air viscosity, $\omega = 2\pi f$ is the angular frequency, *lj* and r_j are the branch length and radius, $i = \sqrt{-1}$, and J_0 and J_1 are the zeroth and first solutions to Bessel's equation.

At the end of each terminal bronchiole, a constant-phase viscoelastic model was used to account for acinar contributions to impedance [17] such that the impedance of each acinar region (Z_{acin}) is given by

$$Z_{acin} = \frac{G - iH}{N\,\omega^{\alpha}},$$

where G and H are coefficients for tissue damping and elastance respectively, N is the total number of terminal bronchioles in the structure, and

$$\alpha = \frac{2}{\pi} tan^{-1}\left(\frac{H}{G}\right).$$

The parameters G and H were taken from standard values in the literature [20] as 0.12 and 0.57 kPa.L^{-1} respectively.

The total impedance of the branch structure was calculated by summing up the impedances of each branch and acinar region in series and parallel, analogous to an electrical circuit. Alongside the total airway tree impedance, chest wall, tracheal, and glottal resistances (taken as 0.049kPa.s.L^{-1}), and chest wall elastance (taken as 1.04kPa.s.L^{-1}) were added in series to the airway tree, parameterised from mean population clinical measurements[21]. Finally, upper airway and cheek shunting were added in parallel to the rest of the model. The shunt data was taken from the

literature[22] , and interpolated using least-squares with the models $R = a/(b + f)$ and $X = c\,log(f) + d$, where a, b, c, and d are the data-fitting parameters.

To aid interpretation, in **Figure OS.1** we give a diagram of the key components of the computational model procedure. As shown in the figure, CT scans (A) are used to generate a virtual representation of the upper airways and algorithmic generation to generate the remainder of the conducting zone structure (B). Each branch in this structure is assumed to have an impedance *Z*, calculated by solving the wave equation in a cylindrical conduit. Total impedance of the airways is calculated by summation of branch impedances in parallel and series (C), with each branch being subtended by a constant-phase respiratory zone impedance. The conducting zone and respiratory zone impedance curves are added in series to tracheal and chest wall impedances, and in parallel to cheek shunting (D), to give total impedance. This leads to the simulation of resistance (E) and reactance (F) curves over the desired frequency range.

Supplement 3 – Summaries and stratification of the asthmatic cohort

Figure 4 in the main manuscript presented a summary of analysis and stratification of the large asthmatic cohort, based on R5-R20 measurements, and spirometric measurements. Here we provide summary statistics, and analysis of the data.

In **Table OS.1** we present summary statistics of the clinical data from the asthmatic cohort. This data has been stratified according to spirometric values, specifically on their forced vital capacity (FVC) Z score, and whether FEV_1/FVC is less than the lower limit of normality. Patients with abnormal FVC are shown in group 1 [FVC Z score < -1.64 (n=30)]; patients with normal FVC but abnormal FEV_1/FVC in group 2 [FVC Z score ≥ -1.64 but FEV_1/FVC < LLN (n=52)] and

AJRCCM Articles in Press. Published on 18-May-2019 as 10.1164/rccm.201812-2322OC

patients with normal spirometry, in group 3 [FVC Z score ≥ -1.64 and FEV1/FVC ≥ LLN (n=95)], 11/95 patients within group 3 had evidence of 'early small airways disease' with an R5-R20 > 100% predicted, as represented schematically on **Figure 4 (**main manuscript).

Patients in group 1 have significantly poorer asthma outcomes, measured with ACQ-6 (p=0.002) and higher number of exacerbations (p<0.0001), compared with patients with normal spirometry and abnormal FEV_1/FVC ratio alone. Additionally, this group presented significantly higher values for R5, R20 and R5-R20. The median R5-R20 was significantly lower in the early disease group compared to groups 1 and 2 (0.05 Kpa.s.L^{-1}, p<0.0001). Nonetheless, as seen in **Figure 4** (main manuscript), 12% of patients in this group have isolated small airways disease, in the presence of normal spirometric indices. To analyse group 3 further (to help detect early signs of small airways disease) we split the group into two subsets, 3A: patients with a normal R5-R20; 3B: patients with R5-R20 > 100% of predicted (11 cases in total). Within **Figure OS.2 we** compare spirometric and oscillometric responses of this group, indicating the occurrence of abnormal R5-R20 in the presence of normal spirometric measurements (A). Additionally, panels B, C and D population show asthma outcomes and exacerbations across the three groups. The number of exacerbations per year is significantly higher in the subset with abnormal R5-R20 (p=0.036). Additionally ACQ-6 and AQLQ show a similar but non-significant trends for worst outcomes for subset 3B.

Table OS.1: Clinical Characteristics of the asthma population

	Group 1: (n = 30) **FVC Z score < - 1.64**	**Group 2: (n=52)** **FEV_1/FVC < LLN & FVC Z score≥-1.64**	**Group 3: (n=95)** **FEV_1/FVC≥ LLN & FVC Z score ≥ -1.64**	**Kruskal-Wallis p-value**
Age (years)	60 (45-65)	58 (47-64)	56 (45-65)	0.734
Sex [% male (n)][b]	53 (16)	54 (28)	40 (38)	0.250
BMI (kg/m^2)	28 (24-34)	27 (23-30)	28 (25-32)	0.200
Smoking pack year history	0 (0-0)¥	0 (0-4)	0 (0-2)	0.039
GINA treatment step (number per group: 1, 2-4, 5)[b]	2, 14, 14	4, 28, 20	11, 67, 17	0.007
ACQ-6	1.83 (0.77-3.07)	1.62 (0.83-2.79)	1.14 (0.58-1.71)Δ,µ	0.002
AQLQ	5.19 (3.67-5.94)	5.62 (3.76-6.27)	5.67 (4.78-6.31)	0.052
Exacerbations (year prior to visit 1)	3 (1-4)	1 (0-3)	1 (0-3)	<0.0001
GLI-FEV_1 Z score	-2.82 (-3.37- -2.27) Δ,¥	-1.91 (-2.46- -1.26)	-0.43 (-1.02-0.37)µ	<0.0001
R5 ($kPa.s.L^{-1}$)	0.52 (0.42-0.63) Δ	0.48 (0.33-0.58)	0.39 (0.31-0.47) µ	<0.0001
R5 % predicted (95^{th} percentile)	117 (96-162)Δ	105 (85-139)	88 (74-106)µ	<0.0001
R20 ($kPa.s.L^{-1}$)	0.35 (0.31-0.48)	0.35 (0.29-0.44)	0.33 (0.28-0.38)	0.061
R20 % predicted (95^{th} percentile)	108 (91-135)Δ	103 (88-123)	91 (79-106)µ	0.0017

AJRCCM Articles in Press. Published on 18-May-2019 as 10.1164/rccm.201812-2322OC

R5-R20 (kPa.s.L^{-1})	0.15 (0.07-0.21)Δ	0.09 (0.04-0.18)	0.05 (0.03-0.09)µ	<0.0001
R5-R20 % predicted (95th percentile)	100 (48-143)Δ	70 (25-116)	38 (23-66)µ	<0.0001

Legend: R5-R20: Resistance at 5 Hz minus resistance at 20 Hz; LLN: Lower limit of normal; BMI: Body Mass Index; ACQ: Asthma control questionnaire; AQLQ: Asthma quality of life questionnaire; FEV_1: Forced expiratory volume in one second; FVC: Forced vital capacity; Z-FEV_1 = Global lung Initiative (GLI) Z score; R5-R20: Resistance at 5 Hz minus resistance at 20 Hz. Data expressed as median (Q1-Q3). **b**: χ^2 test p value. Δ p<0.05 group 1 vs group 3; µ p<0.05 group 2 vs group 3; ¥ p<0.05 group 1 vs group 2.

Supplement 4 – Comparison of resistive difference frequency points.

The key hypothesis of this study is that low-high frequency resistive difference could be a valuable marker of small airways dysfunction in the human lungs. The definition of such a marker necessitates the choice of which frequency is 'low' and which is 'high'. Due to their prevalence within the literature, we have chosen 5Hz and 20Hz as the low and high points respectively. However, for completeness, we briefly analyse the broader spectrum of potential markers within the 5-35Hz range.

We first introduce the notation Rf, to denote the total lung resistance in response to a pressure frequency f. The low-high resistive difference between two frequencies f_1 and f_2 is then: $Rf_1 - Rf_2$.

The best choice of low and high point is one which most significantly amplifies the resistive difference under small airways constriction, while minimising the response under central airways constriction. To identify this choice, we define the index:

$$\Delta Rf_1f_2 = \frac{1}{Rf_1}\left([Rf_1 - Rf_2]_{small} - [Rf_1 - Rf_2]_{central}\right).$$

Where subscripts 'small', and 'central' denote the marker response under 50% constriction of the small and central airways respectively (using the same constriction procedure as in **Figure 2e-f**). This index is normalised by the baseline low resistance Rf_1, to account for larger frequency ranges naturally leading to larger resistive difference.

In **Figure OS.3** we illustrate the values of ΔRf_1f_2 for a range of choices of f_1, and with $f_2 = f_1 + 1, f_1 + 2, \ldots, 35$. As can be seen, the largest values of ΔRf_1f_2 occur when $f_1 = 5$Hz, and $f_2 =$ 20-25Hz. This suggests that the marker we have chosen (R5-R20) is particularly effective at isolating small airways dysfunction, comparative to most other choices. However, it also suggests that similar utility could be found in similar markers such as R5-R25.

Supplement 5 – Analysis of skew-normally distributed airway constrictions

Within the main manuscript we presented a series of results which analysed the response of R5-R20 to constriction of the small and central airways. These constrictions were applied either homogeneously (constricting each branch by the same amount) or heterogeneously, drawing each constriction from a normal distribution, with a fixed mean μ, and standard deviation 0.2 μ. While comparison of these two cases illustrated qualitatively similar response patterns, these are not the only potential ways that constrictions could be applied.

In particularly, given the non-linear relationship between smooth muscle contraction and airway shortening, it could be argued that a skewed normal distribution is more representative of asthma

AJRCCM Articles in Press. Published on 18-May-2019 as 10.1164/rccm.201812-2322OC

than a standard normal distribution. To investigate this, we first define the skew-normal distribution, through the probability density function (pdf):

$$pdf(\mu,\sigma,\alpha) = \frac{2}{\sqrt{2\pi\sigma^2}} e^{-\frac{(x-\mu)^2}{2\sigma^2}} \int_{-\infty}^{\frac{x-\mu}{\sigma}\alpha} \frac{1}{\sqrt{2\pi}} e^{-t^2/2} dt$$

where μ and σ and the mean and standard deviation of the original normal distribution, and α is the degree of applied skew.

To illustrate the effect of the skewing, we recreate the results in **Figure 2c-f**, using the skew-normal distribution. Constrictions were applied to either an entire Strahler order (1-12), all small airways (1-6) or all central airways (7-10). Like the original simulations, constrictions were applied using a mean constriction rate μ ($\mu = 0.05,..., 0.65$), with $\sigma = 0.2\mu$. The constrictions were applied using either a strong leftward skew ($\alpha = -4$), or rightward skew ($\alpha = 4$). As with the original simulations, a constriction rate that exceed 95% was floored to this value to avoid non-physical scenarios.

In **Figure OS.4** we show the response of R5-R20 to both negative and positive skew-normally distributed constrictions. We note that while specific index values are different to those seen in **Figure 2c-f**, the overall trend is qualitatively the same. In both cases, the response of the index to small airways constriction is greater than the response to central airways constriction, with peak values occurring around constriction of Strahler order 6-7.

REFERENCES

(1) Juniper EF, Svensson K, Mörk AC, Ståhl E. Measurement properties and interpretation of three shortened versions of the asthma control questionnaire. *Respir Med*, **99**(5): 553-8 (2005).

(2) Juniper EF, *et al*. Validation of a standardized version of the Asthma Quality of Life Questionnaire. *Chest,* **115**(5): 1265-1270 (1999).

(3) Oostveen E, *et al*. The forced oscillation technique in clinical practice: methodology, recommendations and future developments. *Eur Respir J*, **22**(6):1026-41 (2003).

(4) Miller MR, et al. Standardisation of spirometry. *Eur Respir J*, **26**(2):319-38 (2005).

(5) Galant SP, Komarow HD, Shin HW, Siddiqui S, Lipworth BJ. The case for impulse oscillometry in the management of asthma in children and adults. *Ann Allergy Asthma Immunol*, **118**(6):664-71 (2017).

(6) Schulz H, *et al*. Reference values of impulse oscillometric lung function indices in adults of advanced age. PloS one, **8**(5):e63366 (2013).

(7) Hozawa S, Terada M, Hozawa M. Comparison of budesonide/formoterol Turbuhaler with fluticasone/salmeterol Diskus for treatment effects on small airway impairment and airway inflammation in patients with asthma. *Pulm pharmacol Ther*., **24**(5):571-6 (2011).

(8) Hozawa S, Terada M, Hozawa M. Comparison of the effects of budesonide/formoterol maintenance and reliever therapy with fluticasone/salmeterol fixed-dose treatment on airway inflammation and small airway impairment in patients who need to step-up from inhaled corticosteroid monotherapy. *Pulm Pharmacol Ther*, **27**(2):190-6 (2014).

AJRCCM Articles in Press. Published on 18-May-2019 as 10.1164/rccm.201812-2322OC

(9) Hozawa S, Terada M, Haruta Y, Hozawa M. Comparison of early effects of budesonide/formoterol maintenance and reliever therapy with fluticasone furoate/vilanterol for asthma patients requiring step-up from inhaled corticosteroid monotherapy. *Pulm Pharmacol Ther*, **37**:15-23 (2016).

(10) Hoshino, M. Comparison of effectiveness in ciclesonide and fluticasone propionate on small airway function in mild asthma. *Allerg Int*, ***59***(1): 59-66 (2010).

(11) Yamaguchi, M, Niimi, A, Ueda, T, Takemura, M, Matsuoka, H, Jinnai, M, Otsuka, K, Oguma, T, Takeda, T, Ito, I, & Matsumoto H. Effect of inhaled corticosteroids on small airways in asthma: investigation using impulse oscillometry. *Pulm Pharm & Therap.* **22(4)**, 326-332.

(12) Gonem S, *et al*. Clinical significance of small airway obstruction markers in patients with asthma. *Clin Exp Allergy*, **44**(4):499-507 (2014)

(13) Bordas R, Lefevre C, Veeckmans B, Pitt-Francis J, Fetita C, Brightling CE, Kay D, Siddiqui S, Burrowes KS. Development and analysis of patient-based complete conducting airways models. PloS one. 2015 Dec 11;10(12):e0144105.

(14) Tawhai MH, Pullan AJ, Hunter PJ. Generation of an anatomically based three-dimensional model of the conducting airways. Ann Biomed Eng. 2000 Jul 1;28(7):793-802.

(15) Tawhai MH, Hunter P, Tschirren J, Reinhardt J, McLennan G, Hoffman EA. CT-based geometry analysis and finite element models of the human and ovine bronchial tree. J Appl Physiol. 2004 Dec 1;97(6):2310-21.

(16) Kaczka DW, Massa CB, Simon BA. Reliability of estimating stochastic lung tissue heterogeneity from pulmonary impedance spectra: a forward-inverse modeling study. Ann Biomed Eng. 2007 Oct 1;35(10):1722-38.

(17) Lutchen KR, Gillis H. Relationship between heterogeneous changes in airway morphometry and lung resistance and elastance. J App Physiol, 83(4): 1192-1201, 1997.

(18) Benade AH. On the propagation of sound waves in a cylindrical conduit. J. Acoust. Soc. Am 44(2): 616-623, 1968.

(19) Thurston GB. Periodic fluid flow through circular tubes. J. Acoust. Soc. Am 24(6): 653-656, 1952.

(20) Kaczka DW, Ingenito, EP, Suki, B, Lutchen KR. Partitioning airway and lung tissue resistances in humans: effects of bronchoconstriction. J App Physiol, 82(5) 1531-1541. 1997.

(21) Bhatawedakar, SA, Leary, D, Maksym GN. Modelling resistance and reactance with heterogeneous airway narrowing in mild to severe asthma. Can. J. Physiol. Pharmacol 93.3 (2015): 207-214.

(22) Cauberghs, M, Van de Woestijne, KP. Mechanical properties of the upper airway. J App Physiol. 55(2), 335-342.

AJRCCM Articles in Press. Published on 18-May-2019 as 10.1164/rccm.201812-2322OC

FIGURE LEGENDS

Figure OS.1: Diagram of the integrated FOT modelling approach. Patient specific CT scan data (A) is used to create patient-based virtual airway structures (1) (to generations 6-10), with the remainder of the small conducting airways being generated algorithmically (2) (B). These structures then have patient-specific impedances calculated through an electrical circuit analogous model (C), which is connected to global models for tracheal and chest wall contributions, and cheek shunting (D). This allows for the effective simulation of resistance (E) and reactance (F) curves across the desired frequency range.

Figure OS.2: Population stratification and clinical outcomes in patients with normal spirometry. (A) Dot plot presenting study population according to spirometric outcomes (grey: spirometry strata with gas trapping, asthma/COPD overlap in figure 4: main manuscript). (B-D) Data presented for patients in the normal spirometry stratum (FVC≥ LLN and FEV_1/FVC ≥LLN) for patients with R5-R20 ≤ 100% predicted (green) and R5-R20 > 100% predicted (red): ACQ-6 (B), AQLQ(C) and exacerbations (D). Data are presented as median (Q1-Q3).

Figure OS.3: Analysis of low and high points for the resistive difference index. Plots of the maximum index value (ΔRij) are given, using i = 5, 8, 10, 12, 15, 18, and 20Hz. For each choice of low point, the high point varies from i+1 to 35Hz. As can be seen, the largest index values occur when i = 5Hz, and j = 20-25Hz, corresponding to markers such as R5-R20, and R5-R25.

Figure OS.4: Comparison of R5-R20 response under skew-normally distributed constrictions. Responses are given for constriction of single Strahler orders (C, D), and of all the

small and central airways (E, F) for negatively skewed (A) and positively skewed (B) distributions. In all cases, R5-R20 is largest when constricting the small airways (Strahler orders 1-6).

AJRCCM Articles in Press. Published on 18-May-2019 as 10.1164/rccm.201812-2322OC

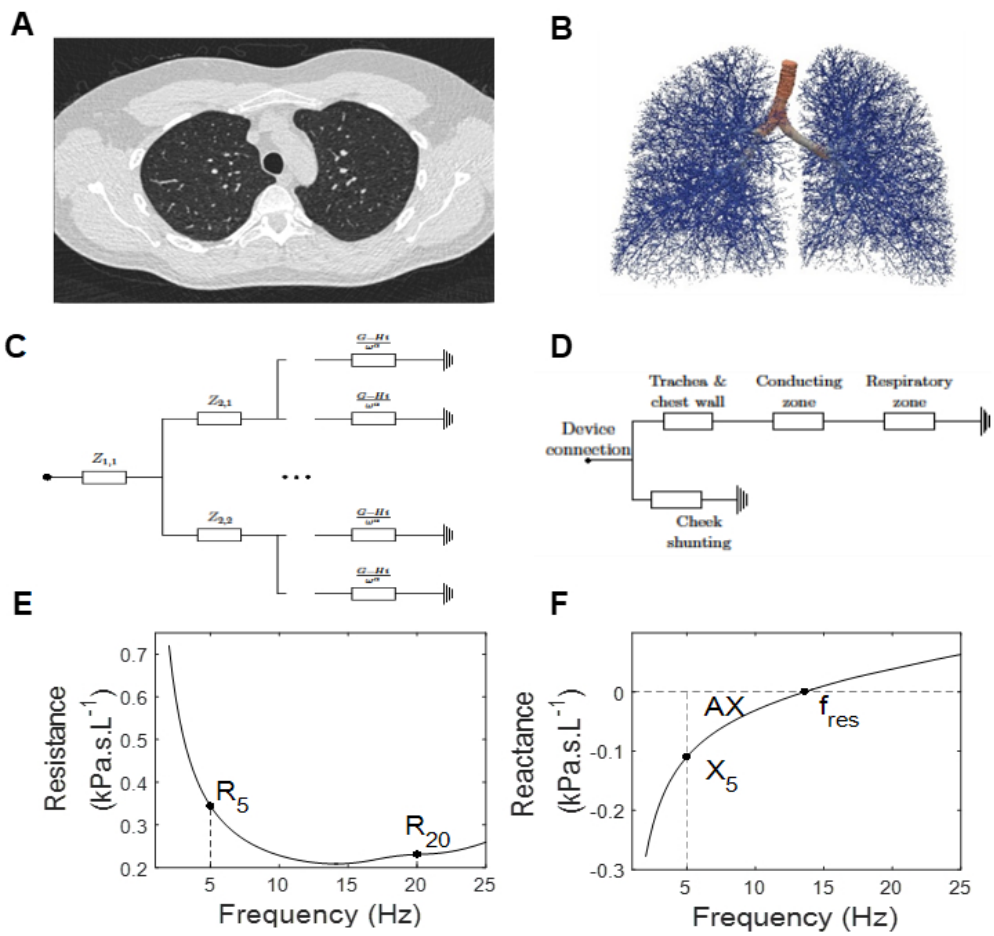

Figure OS.1: Diagram of the integrated FOT modelling approach. Patient specific CT scan data (A) is used to create patient-based virtual airway structures (1) (to generations 6-10), with the remainder of the small conducting airways being generated algorithmically (2) (B). These structures then have patient-specific impedances calculated through an electrical circuit analogous model (C), which is connected to global models for tracheal and chest wall contributions, and cheek shunting (D). This allows for the effective simulation of resistance (E) and reactance (F) curves across the desired frequency range.

191x178mm (96 x 96 DPI)

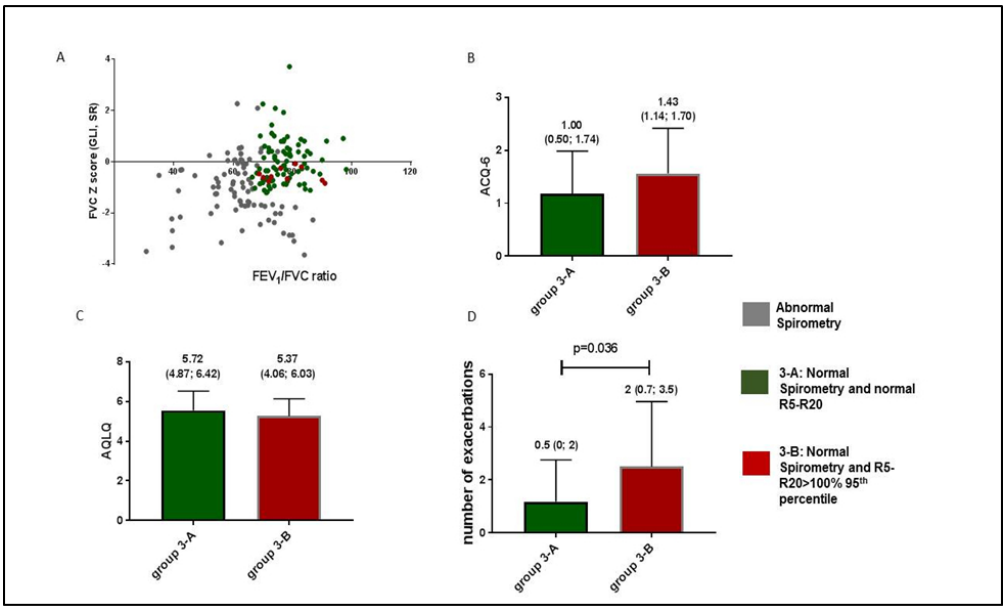

Figure OS.2: Population stratification and clinical outcomes in patients with normal spirometry. (A) Dot plot presenting study population according to spirometric outcomes (B-D) Data presented for patients in the normal spirometry stratum (FVC≥ LLN and FEV1/FVC ≥LLN) for patients with R5-R20 ≤ 100% predicted (green) and R5-R20 > 100% predicted (red): ACQ-6 (B), AQLQ(C) and exacerbations (D). Data are presented as median (Q1-Q3).

258x157mm (96 x 96 DPI)

AJRCCM Articles in Press. Published on 18-May-2019 as 10.1164/rccm.201812-2322OC

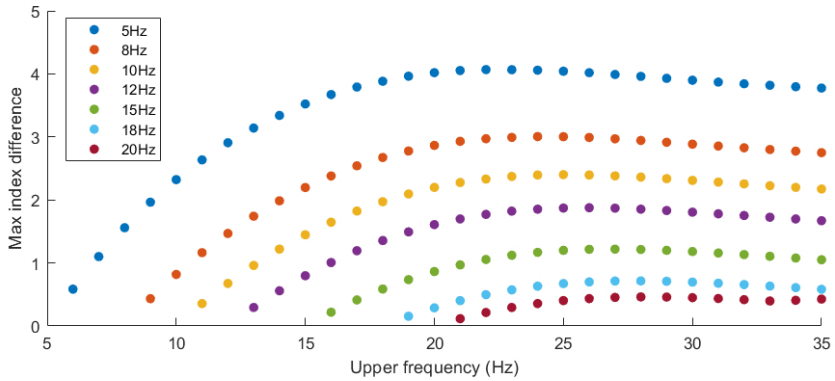

Figure OS.3: Analysis of low and high points for the resistive difference index. Plots of the maximum index value (ΔRij) are given, using i = 5, 8, 10, 12, 15, 18, and 20Hz. For each choice of low point, the high point varies from i+1 to 35Hz. As can be seen, the largest index values occur when i = 5Hz, and j = 20-25Hz, corresponding to markers such as R5-R20, and R5-R25.

274x109mm (96 x 96 DPI)

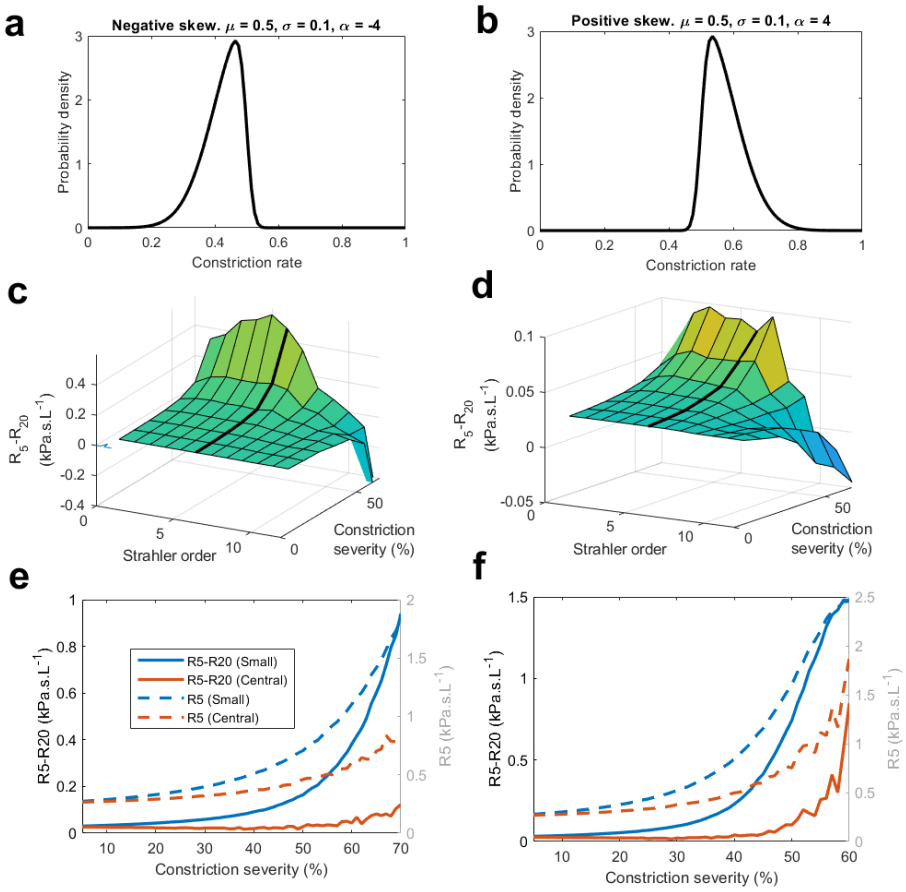

Figure OS.4: Comparison of R5-R20 response under skew-normally distributed constrictions. Responses are given for constriction of single Strahler orders (C, D), and of all the small and central airways (E, F) for negatively skewed (A) and positively skewed (B) distributions. In all cases, R5-R20 is largest when constricting the small airways (Strahler orders 1-6).

287x264mm (96 x 96 DPI)